

## MIT Open Access Articles

*SCARB2/LIMP-2 Regulates IFN Production of Plasmacytoid Dendritic Cells by Mediating Endosomal Translocation of TLR9 and Nuclear Translocation of IRF7*

The MIT Faculty has made this article openly available. **Please share** how this access benefits you. Your story matters.

**Citation:** Guo, Hao et al. "SCARB2/LIMP-2 Regulates IFN Production of Plasmacytoid Dendritic Cells by Mediating Endosomal Translocation of TLR9 and Nuclear Translocation of IRF7." The Journal of Immunology 194.10 (2015): 4737–4749.

**As Published:** <http://dx.doi.org/10.4049/jimmunol.1402312>

**Publisher:** American Association of Immunologists

**Persistent URL:** <http://hdl.handle.net/1721.1/106316>

**Version:** Author's final manuscript: final author's manuscript post peer review, without publisher's formatting or copy editing

**Terms of use:** Creative Commons Attribution-Noncommercial-Share Alike





Published in final edited form as:

*J Immunol.* 2015 May 15; 194(10): 4737–4749. doi:10.4049/jimmunol.1402312.

## SCARB2/LIMP-2 Regulates IFN Production of Plasmacytoid Dendritic Cells by Mediating Endosomal Translocation of TLR9 and Nuclear Translocation of IRF7

Hao Guo<sup>\*†</sup>, Jialong Zhang<sup>\*</sup>, Xuyuan Zhang<sup>\*†</sup>, Yanbing Wang<sup>\*</sup>, Haisheng Yu<sup>\*†</sup>, Xiangyun Yin<sup>\*†</sup>, Jingyun Li<sup>\*†</sup>, Peishuang Du<sup>\*</sup>, Joel Plumas<sup>‡</sup>, Laurence Chaperot<sup>‡</sup>, Jianzhu Chen<sup>\*§¶</sup>, Lishan Su<sup>\*||#</sup>, Yongjun Liu<sup>\*\*</sup>, and Liguozhang<sup>\*</sup>

<sup>\*</sup>Key Laboratory of Immunity and Infection, Institute of Biophysics, Chinese Academy of Sciences, Beijing, BJ 100101, China

<sup>†</sup>University of Chinese Academy of Sciences, Beijing, BJ 100080, China

<sup>‡</sup>Department of Research and Development, Etablissement Français du Sang Rhône-Alpes Grenoble, La Tronche 38701, France

<sup>§</sup>Koch Institute for Integrative Cancer Research, Massachusetts Institute of Technology, Cambridge, MA 02139

<sup>¶</sup>Department of Biology, Massachusetts Institute of Technology, Cambridge, MA 02139

<sup>||</sup>Lineberger Comprehensive Cancer Center, University of North Carolina at Chapel Hill, Chapel Hill, NC 27599

<sup>#</sup>Department of Microbiology and Immunology, University of North Carolina at Chapel Hill, Chapel Hill, NC 27599

<sup>\*\*</sup>Baylor Institute for Immunology Research, Baylor Research Institute, Dallas, TX 75204

### Abstract

Scavenger receptor class B, member 2 (SCARB2) is essential for endosome biogenesis and reorganization and serves as a receptor for both  $\beta$ -glucocerebrosidase and enterovirus 71. However, little is known about its function in innate immune cells. In this study, we show that, among human peripheral blood cells, SCARB2 is most highly expressed in plasmacytoid dendritic cells (pDCs), and its expression is further upregulated by CpG oligodeoxynucleotide stimulation. Knockdown of SCARB2 in pDC cell line GEN2.2 dramatically reduces CpG-induced type I IFN production. Detailed studies reveal that SCARB2 localizes in late endosome/lysosome of pDCs, and knockdown of SCARB2 does not affect CpG oligodeoxynucleotide uptake but results in the retention of TLR9 in the endoplasmic reticulum and an impaired nuclear translocation of IFN regulatory factor 7. The IFN-I production by TLR7 ligand stimulation is also impaired by

---

Address correspondence and reprint requests to Prof. Liguozhang, Institute of Biophysics, Chinese Academy of Sciences, 15 Da Tun Road, Chaoyang District, Beijing, BJ 100101, China. [liguozhang@ibp.ac.cn](mailto:liguozhang@ibp.ac.cn).

The online version of this article contains supplemental material.

### Disclosures

The authors have no financial conflicts of interest.

SCARB2 knockdown. However, SCARB2 is not essential for influenza virus or HSV-induced IFN-I production. These findings suggest that SCARB2 regulates TLR9-dependent IFN-I production of pDCs by mediating endosomal translocation of TLR9 and nuclear translocation of IFN regulatory factor 7.

---

Lysosomes are ubiquitous acid membrane-bound organelles involved in the degradation of molecules, complexes, and structures that enter the endocytic pathway through endocytosis, phagocytosis, or autophagy (1–3). More than 25 integral lysosomal membrane proteins (LMPs) have been identified to play critical roles in maintaining the morphology and function of lysosomes in mammals (4). The most abundant LMPs discovered to date are lysosome-associated membrane protein (LAMP)-1, LAMP-2, scavenger receptor class B, member 2 (SCARB2), and CD63.

SCARB2, also known as lysosome integral membrane protein-2 or LGP85, belongs to the CD36 superfamily of scavenger receptors, which also includes scavenger receptor class B, member 1 (SCARB1), and CD36 (5). SCARB2 is a highly glycosylated type III membrane protein residing in the membrane of late endosome and lysosome (6, 7). The endosome and lysosome targeting of SCARB2 is mediated by a di-leucine-based motif “DERAPLI” in the C-terminal cytoplasmic tail (8, 9). And the adaptor protein complexes (AP)-1 and AP-3 help to sort SCARB2 from *trans* Golgi network to late endosome/lysosome (10, 11).

Based on studies in macrophages and a small number of cell lines, various functions have been attributed to SCARB2 (12–14). As an abundant LMP, SCARB2 plays a critical role in the biogenesis and reorganization of endosomes and lysosomes. Over-expression of SCARB2 in mammalian cells results in direct disturbance of membrane trafficking and accumulation of cholesterol, which leads to enlargement of endosomal/lysosomal compartments (12, 15). SCARB2 has been reported to transport  $\beta$ -glucocerebrosidase ( $\beta$ -GC), a lysosomal hydrolase whose mutation might cause lysosomal storage disorder Gaucher disease (GD), from endoplasmic reticulum (ER) to lysosome (16). Recently, SCARB2 has been shown to serve as a receptor for enterovirus 71 and coxsackievirus A16, the major viruses that cause hand-foot-and-mouth disease (13, 17, 18). These findings suggest that SCARB2 is a critical lysosomal protein involved in diverse functions of endocytic processes.

However, it is worth noting that almost all those previous studies were carried out in mouse macrophages or cell lines (12, 14, 19), whereas human SCARB2 has a more extensive expression profile in a range of cell types. Based on a cDNA microarray data, we found that SCARB2 was highly expressed in human plasmacytoid dendritic cells (pDCs) compared with other peripheral blood cell types. This raises the question of what is the function of SCARB2 in pDCs.

pDCs are a specialized subset of dendritic cells with extraordinary capacity to produce type I IFN (IFN-I) in response to stimulation by viruses or nucleic acids (20, 21). TLR7 and TLR9 are expressed in pDCs as pattern recognition receptors (PRRs). TLR7 and TLR9 are synthesized in ER (22), where they associate with the ER membrane protein uncoordinated 93 homolog B1 and traffic through Golgi to endolysosomes (23–26). During this process,

AP-3 mediates the translocation of TLR7 and TLR9 into lysosomes or lysosome-related organelles (27). In these acid compartments, TLR7 and TLR9 undergo proteolytic processing by cathepsins and asparagine endopeptidase to become functionally competent receptors (28, 29). After that, those PRRs can recognize, respectively, ssRNA or dsDNA and initiate IFN-I signaling pathway.

As important stimulators for pDCs, different classes of CpG oligodeoxynucleotides (CpG-ODNs) with distinct primary sequence motifs and secondary and tertiary structures have been generated. The most commonly used CpG-ODNs are CpG A and CpG B. The former induces high levels of IFN- $\alpha$ , but has poor activity in inducing pDC differentiation. However, the latter induces stronger pDC maturation, but weaker IFN- $\alpha$  secretion (30, 31). In brief, upon stimulation by those ligands, both TLRs recruit the cytoplasmic adaptor MyD88 and initiate downstream signaling cascade, involving TNFR-associated factor 6, IL-1R-associated kinase, inhibitor of  $\kappa$ B kinase- $\alpha$ , and IFN regulatory factor (IRF) 7. Eventually, IRF7 is phosphorylated and transported into the nuclei to initiate IFN-I transcription (31–34). Activated pDCs can also secrete TNF- $\alpha$ , IL-6, and chemokines as well as upregulate the expression of MHC and costimulatory molecules to present Ags to T cells (21, 35). Thus, pDCs play a crucial role in bridging the innate and adaptive immunity.

To our knowledge, there is no previous report on the specific functions of SCARB2 in human pDCs. Thus, we have used primary pDCs and pDC cell line GEN2.2 to investigate SCARB2's expression and function. In this work, we show that SCARB2 is expressed in late endosome/lysosome of pDCs at a very high level. Upon activation, SCARB2 expression is further upregulated without changing its subcellular location. Knockdown of SCARB2 in GEN2.2 cells results in the ER retention of TLR9, reduction of IRF7 nuclear translocation, and dramatic inhibition of IFN- $\alpha$  expression. SCARB2 also regulates TLR7-dependent IFN- $\alpha$  production, but has no influence on antiviral IFN-I response. These findings suggest that SCARB2 regulates TLR9-dependent IFN-I production of pDCs by mediating endosomal translocation of TLR9 and nuclear translocation of IRF7.

## Materials and Methods

### Reagents and Abs

Synthesized CpG-ODNs were purchased from Takara and Invitrogen. The sequences of CpG-ODNs were as follows: CpG A (ODN2216), 5'-ggGGGACGATCGTCgggggg-3'; CpG B (ODN2006), 5'-tcgtcgtttgtcgt-tttgtcgtt-3'.

Lowercase letters in CpG-ODN sequences refer to nucleotides for which the 3' internucleotide linkage is phosphorothioate modified, and uppercase letters refer to standard phosphodiester-linked nucleotides. The 5'-biotin-CpG A and 5'-biotin-CpG B were purchased from Takara and Invitrogen, respectively, with biotin labeled at the 5' internucleotide.

mAb against SCARB2 designated as JL-1 was raised in mice that were immunized by L cells transfected with human SCARB2 gene using the standard techniques. For FACS analysis, JL-1 mAb was directly labeled with FITC in Tianjin Sungene Biotech (Tianjin,

China) and designated as JL-1-FITC. All of the other Abs used in this work are listed in Supplemental Table 1.

### Cell culture

The human embryonic kidney cell line HEK293T was cultured in a 5% CO<sub>2</sub> incubator at 37°C with complete DMEM (Life Technologies) supplemented with 10% FBS (Hyclone, Thermo Fisher Scientific), L-glutamine (Invitrogen), and penicillin/streptomycin (Invitrogen).

GEN2.2 cells were cultured in GlutaMax-RPMI 1640 (Life Technologies) supplemented with 10% FBS (Life Technologies), L-glutamine (Invitrogen), MEM-nonessential amino acid solution (Life Technologies), penicillin/streptomycin (Invitrogen), and sodium pyruvate (Invitrogen).

### Plasmid construction, lentivirus production, and stable cell line generation

pLKO.1 vectors encoding short hairpin RNA (shRNA) for a scrambled molecule or SCARB2 were purchased from Open Biosystem, and then the shRNA sequences were subcloned into FG12 vectors.

FG12-shRNA vectors were transfected into HEK293T cells together with NRF (a packaging plasmid) and vesicular stomatitis virus G (an envelope plasmid) for producing viral particles using the standard calcium phosphate techniques. Culture supernatants were harvested 24 and 48 h after transfection and then centrifuged at 2000 rpm for 10 min. GEN2.2 cells were infected with collected supernatants containing lentiviral particles in the presence of 4 mg/ml polybrene (Sigma-Aldrich). As a GFP gene existing in the FG12 vector, after 48 h of culture, lentiviral-infected cells with GFP expression were sorted with BD FACS AriaII (BD Biosciences). Gene-targeting efficiencies of each shRNA-targeted molecule were verified by real-time PCR and/or Western blotting analysis.

### Flow cytometry analysis and purification

PBMCs of healthy volunteers were isolated by density gradient centrifugation using Ficoll-Paque Plus (17-1440-02; GE Healthcare). Then PBMCs were washed twice with PBS plus 2% FBS and 2 mM EDTA and blocked with 10% human serum plus 10% goat serum. Whereafter, they were stained with anti-human BDCA2-PE, anti-human CD123-PerCP/Cy5.5, and 7-aminoactinomycin D and then permeabilized with a Perm/Wash buffer (554723; BD Biosciences). Finally, intracellular SCARB2 was detected by JL-1-FITC.

SCARB2 expression in GEN2.2 cells was also detected, as described above.

Primary pDCs were purified from PBMCs by staining with anti-human BDCA2-PE and anti-human CD123-PerCP/Cy5.5 and sorting with a FACS AriaII flow cytometer (BD Biosciences). Reanalysis of the sorted cells confirmed a purity of >98%.

To observe SCARB2 expression in primary pDCs upon stimulation, purified pDCs were cultivated in presence of 10 ng/ml IL-3 (200-03; PeproTech) alone or together with 1 μM

CpG A or 0.2  $\mu$ M CpG B for 20 h. Cells were harvested, washed, permeabilized, and blocked. After that, they were stained with JL-1-FITC (anti-SCARB2).

To observe the uptake of CpG-ODNs, SCARB2 knockdown (sh-1) and control cells (sh-c) were incubated with 1  $\mu$ M biotin-conjugated CpG B for 1, 2, and 4 h. Cells were harvested, washed, permeabilized, and blocked. After that, they were stained with JL-1 (anti-SCARB2), followed by PE goat anti-mouse IgG and allophycocyanin streptavidin.

All flow cytometry analysis was conducted on a FACSCalibur flow cytometer (BD Biosciences), and data were analyzed with Summit 4.3 (DAKO).

### mRNA extraction and real-time PCR

For primary cells, purified pDCs were stimulated with 1  $\mu$ M CpG A or 0.2  $\mu$ M CpG B for 20 h in the presence of 10 ng/ml IL-3 (200-03; PeproTech).

For cell lines, GEN2.2 cells were stimulated with 2  $\mu$ M CpG A, 0.2  $\mu$ M CpG B, 4  $\mu$ g/ml R848, or 20  $\mu$ g/ml R837 for the indicated durations.

Total RNA was extracted from fresh or stimulated cells with TRIzol (Invitrogen), according to the manufacturer's instructions. Oligo(dT) primers and Moloney murine leukemia virus reverse transcriptase (M1705; Promega) were used for the reverse transcription of purified RNA. All of the gene transcripts were quantified by real-time PCR with SYBR Green QPCR Master Mix (S7563; ABI, Life Technologies) and a Rotor-Gene Corbett 65H0 (Corbett Lifescience). GAPDH or EF1- $\alpha$  was used as a housekeeping control to normalize the amounts of cDNA between each sample. Primers for real-time PCR were synthesized by Invitrogen. Their sequences were as follows: GAPDH, forward, 5'-AGCCACATCGCTCAGACAC-3' and reverse, 5'-GCCCAATACGACCAAATCC-3'; EF1- $\alpha$ , forward, 5'-ATATGGTTCCTGGCAAGCCC-3' and reverse, 5'-GTGGG-GTGGCAGGTATTAGG-3'; SCARB2, forward, 5'-AGCCAATACGTCA-GACAATGC-3' and reverse, 5'-TTGGTAAAAGTGTGGGAAAGACA-3'; IFN- $\alpha$ , forward, 5'-GTGAGGAAATACTTCCAAAGAATCAC-3' and reverse, 5'-TCTCATGATTTCTGCTCTGACAA-3'; IFN- $\beta$ , forward, 5'-TG-TTGTAGCAAACCCTCAAGC-3' and reverse, 5'-ATGAGGTACAGGCC-CTCTGA-3'; and TNF- $\alpha$ , forward, 5'-ACTGAACTTCGGGGTGATCG-3' and reverse, 5'-TGGTGGTTTGCTACGACGTG-3'.

### Immunofluorescence analysis

To observe the location of SCARB2 in primary cells, purified pDCs were washed with PBS plus 2% FBS and 2 mM EDTA, and then permeabilized with a Perm/Wash buffer. After blocking with 10% human serum plus 10% goat serum, the cells were stained with JL-1 (anti-SCARB2) together with early endosome marker anti-transferrin receptor (TfR)-biotin or late endosome marker anti-LAMP-1-AF647, followed by DyLight 549 goat anti-mouse IgG and/or Cy5 streptavidin.

To observe the location of SCARB2 in cell lines, fresh GEN2.2 cells or cells stimulated with 0.2  $\mu$ M CpG B for 20 h were operated by the same method described above.

To observe nuclear translocation of IRF7, SCARB2 knockdown (sh-1) and control cells (sh-c) were stimulated with 0.2  $\mu$ M CpG B for 4 h, respectively. After permeabilization with a Perm/Wash buffer and blocking with 10% goat serum, the cells were stained with anti-IRF7, followed by DyLight 649 goat anti-rabbit IgG. Nuclei were identified using DAPI staining (Sigma-Aldrich).

To observe the uptake of CpG-ODNs, SCARB2 knockdown (sh-1) and control cells (sh-c) were mixed together by equal amounts and incubated with 1  $\mu$ M biotin-conjugated CpG B for 1 h. The cells were harvested, washed, permeabilized, and blocked. After that, they were stained with JL-1 (anti-SCARB2), followed by DyLight 549 goat anti-mouse IgG and Cy5 streptavidin.

To observe the intracellular trafficking of CpG-ODNs, SCARB2 knockdown (sh-1) and control cells (sh-c) were stimulated with 2  $\mu$ M CpG B for 5 min, 1 h, and 3 h. The cells were harvested, washed, permeabilized, and blocked. After that, they were stained with Cy3 streptavidin together with anti-TfR, followed by AF647 goat anti-mouse IgG or anti-LAMP-1-AF647.

To observe the translocation of TLR9 from ER to endosomes, SCARB2 knockdown (sh-1) and control cells (sh-c) were stimulated with 0.2  $\mu$ M CpG B for 4 h. Cells after stimulation were harvested, washed, permeabilized, and blocked. After that, they were stained with anti-TLR9, followed by DyLight 549 goat anti-mouse IgG. Meanwhile, markers used for organelles were as follows: anti-Calnexin followed by DyLight 649 goat anti-rabbit IgG; anti-TfR-biotin followed by Cy5 streptavidin; and anti-LAMP-1-AF647.

The cells were attached to glass slides by a cytospin centrifuge. Slices were sealed by Vectashield Mounting Medium (Vector Labs) with 1.5  $\mu$ g/ml DAPI (Sigma-Aldrich) and then visualized under a confocal microscope (Olympus FV1000). Data were acquired with FV10-ASW 1.7 Viewer (Olympus). Statistical data of IRF7 and TLR9 subcellular translocation were measured double blinded from at least two random fields of view.

### Western blotting

GEN2.2 cells fresh or stimulated with 0.2  $\mu$ M CpG B for the indicated durations were washed twice with cold PBS and lysed in radioimmunoprecipitation assay buffer (0.01 M Tris [pH 8.0], 0.14 M NaCl, 2 mM EDTA, 1% NaDOC, 0.1% SDS, 1% Triton X-100, 1 mM PMSF, and protease inhibitor cocktail tablets [Roche Diagnostics]) on ice for 30 min. All cell lysates were centrifuged at  $13,300 \times g$  for 20 min at 4°C. Then proteins in supernatants were separated by SDS-PAGE and transferred to polyvinylidene difluoride membranes. Nonspecific binding sites were blocked with 3% BSA in PBS containing 0.1% Tween 20. Membranes were then incubated with anti-SCARB2 at 4°C overnight. Ab labeling was shown with HRP-conjugated secondary Abs (Zsbio) and was visualized with Immobilon Western HRP Substrate (Millipore).

Similarly, SCARB2 knockdown efficiencies in SCARB2 knockdown (sh-1/2) and control cells (sh-c) were also detected, as described above.

### Quantification of cytokine production

SCARB2 knockdown (sh-1/2) and control cells (sh-c) were plated at  $2 \times 10^5$  cells/200  $\mu$ l/well in flat-bottom 96-well plates, as described above, and incubated for 0–20 h with or without 2  $\mu$ M CpG A, 0.2  $\mu$ M CpG B, 4  $\mu$ g/ml R848, 20  $\mu$ g/ml R837, 2 multiplicity of infection Flu, or 5 multiplicity of infection HSV. Plates were centrifuged at 1500 rpm/10 min to pellet cells. Supernatants were collected and either assessed immediately or stored at  $-80^\circ\text{C}$ . ELISA was performed to detect human IFN- $\alpha$  (3425-1H-20; MABtech) or IL-6 (3460-1H-20; MABtech), according to the manufacturer's instructions. Absorbance was determined at 450 nm. All samples and standards were measured in duplicates.

### IRF7 nuclear translocation

SCARB2 knockdown (sh-1) and control cells (sh-c) were plated at  $5 \times 10^6$  cells/5 ml in 10-mm dishes, as described above, and incubated for 2 h and 4 h with or without 0.2  $\mu$ M CpG B. Cells were washed twice with cold PBS and lysed in buffer A (10 mM HEPES [pH 7.9], 10 mM KCl, 1.5 mM  $\text{MgCl}_2$ , 0.34 M sucrose, 10% glycerol, 1 mM DTT, 1 mM PMSF, and 0.1% Triton X-100) for 5 min on ice. Samples were centrifuged at  $1300 \times g$  for 4 min at  $4^\circ\text{C}$ . Then the supernatants and pellets were collected separately. The supernatants were centrifuged again at  $17,000 \times g$  for 20 min at  $4^\circ\text{C}$ , and the final supernatants were constituted with soluble cytosolic proteins. Those pellets from the first centrifuge were washed three times with buffer A (without 0.1% Triton X-100) and could be used in Western blotting as nuclear fractions.

All protein samples were immunoblotted using anti-IRF7. Anti-histone H3 and anti-tubulin were used as controls for nuclear and cytosolic fractions separately.

### Statistical analysis

All of the graphs in this work were analyzed by GraphPad Prism software. Data were shown as means  $\pm$  SEM of at least three independent experiments. Statistically significant differences were determined by unpaired, two-tailed, Student *t* test. The *p* values  $< 0.05$  were considered statistically significant.

## Results

### SCARB2 is preferentially expressed in pDCs and localizes in late endosome/lysosome

Based on cDNA array gene expression analysis, we found that SCARB2 was expressed at a much higher level in pDCs than in any other human peripheral blood leukocytes (Fig. 1A). To confirm this result, PBMCs, primary pDCs, and pDC-depleted PBMCs were isolated from healthy volunteers, and the levels of SCARB2 transcript were quantified by real-time PCR analysis (Fig. 1B). Consistent with the microarray data, the level of SCARB2 was  $\sim 7$ -fold higher in pDCs than in total PBMCs. Intracellular staining followed by flow cytometry analysis showed that BDCA2-positive pDCs expressed SCARB2, and the level was the highest among peripheral blood cells (Fig. 1C), whereas direct staining without permeabilization failed to stain SCARB2 on the cell surface (data not shown).



SCARB2 has been reported to localize in the membrane of late endosome and lysosome (8, 9, 16). To determine whether the subcellular distribution of SCARB2 remains the same in human pDCs, primary pDCs were stained with anti-SCARB2 Ab after permeabilization. Confocal microscopy revealed that SCARB2 colocalized with a late endosome/lysosome marker LAMP-1, but not an early endosome marker transferrin receptor (TfR) (Fig. 1D). Considering the paucity and vulnerability of primary pDCs, we carried out some mechanistic studies in GEN2.2 cells, a human leukemic cell line similar to human pDCs both phenotypically and functionally (36). Similar to primary pDCs, SCARB2 was highly expressed in GEN2.2 cells and had a complete colocalization with late endosome marker LAMP-1 (Supplemental Fig. 1). These results show that SCARB2 is highly expressed in human pDCs and localizes in late endosome/lysosome.

### **CpG induces upregulation of SCARB2 expression in pDCs**

SCARB2 is known to play a critical role in the biogenesis of endosome/lysosome and the proper function of endocytic transfer system (12, 37). The high level of SCARB2 expression in pDCs, which are specialized innate immune cells, raises the question of the function of SCARB2 in innate immune responses. To investigate this, we determined whether SCARB2 expression is modulated by TLR stimulation in pDCs. Purified pDCs were cultured in the presence of IL-3 and stimulated with CpG-ODNs, which are TLR9 ligands and stimulate pDCs to produce inflammatory cytokines such as IFN-I (20, 21). Because different CpG-ODNs exhibit different effect on pDCs (30, 31), we used both CpG A and CpG B. As shown in Fig. 2A, the level of SCARB2 transcript was significantly increased following both types of CpG-ODN stimulation. The upregulation of SCARB2 was confirmed at protein level by intracellular staining (Fig. 2B). Similarly, CpG A and CpG B also induced upregulation of SCARB2 in GEN2.2 cells (Fig. 2C). The level of SCARB2 transcript was induced gradually from 8 to 20 h post-CpG B stimulation (Fig. 2C). The upregulation at protein level was also detected by Western blotting (Fig. 2D). Despite the increase of SCARB2 expression, the protein still remained in late endosome/lysosome with a complete colocalization with LAMP-1 (Fig. 2E). These results show that SCARB2 is further upregulated by TLR9 ligands in pDCs, suggesting its role in innate immune responses.

### **SCARB2 regulates TLR9-dependent IFN-I production**

To investigate the function of SCARB2 in human pDCs, we examined the effect of SCARB2 knockdown on production of inflammatory cytokines by GEN2.2 cells following CpG-ODN stimulation. We constructed lentivirus expressing two shRNAs specific for SCARB2 and established stably transduced GEN2.2 cell lines. Quantification of the levels of SCARB2 transcript by real-time PCR and protein by Western blotting in the stable cell lines revealed that the knockdown efficiency was ~90% for one shRNA and 70% for the other (Fig. 3A, 3B). SCARB2 knockdown (sh-1/2) and control cells (sh-c) were then treated with CpG A and CpG B separately, and the secretion of IFN- $\alpha$  and IL-6 was quantified by ELISA. In response to CpG A, IFN- $\alpha$  and IL-6 production showed no difference between SCARB2 knockdown cells and the control cells (Fig. 3C). However, upon CpG B stimulation, SCARB2 knockdown led to ~90% and 40–60% reduction, respectively, in IFN- $\alpha$  and IL-6 production (Fig. 3D). The kinetics of IFN- $\alpha$  transcript by real-time PCR and protein expression was also analyzed. The transient induction of IFN- $\alpha$  transcript was

significantly inhibited in SCARB2 knockdown cells, and expression of IFN- $\alpha$  protein was also remarkably reduced (Fig. 3E). These results might reflect that CpG A and CpG B had distinct pathways to activate pDCs and, somehow, SCARB2 only influenced the mechanism underlying CpG B stimulation (see *Discussion*). We used CpG B as the major agonist in further studies below. In conclusion, these data indicate an important role of SCARB2 in regulating TLR9-dependent IFN-I production in pDCs.

In addition, we stimulated SCARB2 knockdown (sh-1) and control cells (sh-c) with two synthetic TLR7 agonists: R848 and R837. Very low levels of IFN- $\alpha$  secretion were observed at any time point (up to 22 h) after R848 or R837 activation (data not shown), which would be in keeping with many previous findings that the pDC cell line GEN2.2 cells failed to produce significant amounts of type I IFN toward these two ligands because of the transitory activation of inhibitor of  $\kappa$ B kinase- $\beta$  (38, 39). However, SCARB2 knockdown led to a significant reduction in IL-6 production (Supplemental Fig. 2A). Moreover, the transient induction of IFN- $\alpha$ , IFN- $\beta$ , and IL-6 transcript was sharply inhibited in SCARB2 knockdown cells (Supplemental Fig. 2B). These findings suggest that SCARB2 also regulates TLR7-dependent IFN-I production.

### **SCARB2 is not required for virus-induced IFN-I production**

We next investigated the relevance of SCARB2-TLR-IFN pathway in antiviral responses by challenging SCARB2 knockdown (sh-1) and control cells (sh-c) with influenza virus (Flu, RNA virus) and HSV (DNA virus), which could be recognized by TLR7 and TLR9, respectively. Secretion of IFN- $\alpha$  and IL-6 was quantified by ELISA. It was interesting to note that, in response to both viruses, IFN- $\alpha$  and IL-6 production showed no difference between SCARB2 knockdown cells and the control cells (Fig. 4) (see *Discussion*). These results may reflect that SCARB2 is not essential for virus-induced IFN-I production.

### **SCARB2 is essential for TLR9-mediated activation of IRF7**

It is well established that IRF family members are the key transcription factors in regulating IFN-I expression (40, 41). Stimulation of pDCs with CpG-ODNs induces the nuclear translocation of IRF7 after its phosphorylation and dimerization, which eventually mediates IFN- $\alpha$  production (33, 34).

Thus, we examined whether SCARB2 was required for the nuclear translocation of IRF7 upon TLR9-mediated activation. We used CpG B to stimulate SCARB2 knockdown (sh-1) and control cells (sh-c), and then monitored the distribution of IRF7 by Western blotting and immunofluorescence. Nuclear and cytosolic fractions of stimulated cells were isolated and assayed separately. After CpG B stimulation, IRF7 displayed an increased distribution in the nucleus. However, compared with control cells, nuclear translocation of IRF7 was greatly diminished in SCARB2 knockdown GEN2.2 cells (Fig. 5A). This result was further confirmed by confocal microscopy with intracellular staining of IRF7. After 4-h stimulation of CpG B, >70% of control cells showed an IRF7 colocalization with nuclear staining, indicating the nuclear translocation of IRF7 (Fig. 5B, 5C). However, in the case of SCARB2 knockdown cells, IRF7 remained mostly in the cytoplasm with nuclear colocalization in <20% of the cells (Fig. 5B, 5C). These findings suggest that SCARB2 is important for the

activation and nuclear translocation of IRF7 in CpG B-induced TLR9-IRF7-IFN signaling pathway.

### **SCARB2 is not required for CpG B endocytosis and trafficking**

Following CpG-ODN stimulation, the intracellular events resulting in IFN- $\alpha$  production are composed of the following: 1) endocytosis of CpG-ODNs and its trafficking between different endosomes and 2) intracellular translocation of TLR9 (22, 28). We next investigated the possible mechanism(s) from these two aspects.

First, we examined whether SCARB2 knockdown might block the capability of pDCs to uptake CpG-ODNs. To test this hypothesis, we used biotin-conjugated CpG B to stimulate SCARB2 knockdown (sh-1) and control cells (sh-c) for the indicated durations. Intracellular staining of CpG B and SCARB2 followed by flow cytometry analysis showed that the uptakes of CpG B were approximately the same between SCARB2 knockdown and control cells (Fig. 6A). To further confirm this, we mixed SCARB2 knockdown and control cells together at equal ratio, followed by stimulation with biotin-CpG B. The intracellular SCARB2 and CpG B were stained and observed by confocal microscopy. Consistent with the FACS result, SCARB2 knockdown cells endocytosed similar levels of CpG B as control cells, indicating that SCARB2 is not involved in CpG endocytosis (Fig. 6B).

Several studies have demonstrated that the intracellular localization of CpG-ODNs in pDCs strictly correlates with their ability to induce IFN- $\alpha$ . Single-stranded CpG B is quickly transported into late endosome/lysosome and promotes pDC activation (31, 33). To investigate whether an impaired compartmentalization of CpG B could account for the decreased IFN response in SCARB2 knockdown cells, we traced the spatiotemporal trafficking of CpG B using confocal microscopy. We showed that CpG B primarily localized in TfR-positive early endosomes as soon as 1 h upon stimulation (Fig. 6C). However, at this time point, there was also a significant colocalization between CpG B and late endosome marker LAMP-1, implicating a fast routing of CpG B between early and late endosomes (Fig. 6C). Shortly after that, most CpG B localized in LAMP-1-positive endosomal compartments (Fig. 6C). Comparing SCARB2 knockdown (sh-1) cells with control cells (sh-c), no difference was detected in CpG B localization and translocation between early and late endosomes (Fig. 6C). We conclude that SCARB2 is dispensable for CpG endocytosis and translocation.

### **SCARB2 is required for translocation of TLR9 from ER to late endosomes**

We next investigated whether SCARB2 participated in TLR9's translocation toward endosomes, a prerequisite for TLR9-IFN signaling (22, 23, 28). To address this question, we first examined the intracellular distribution of TLR9 in GEN2.2 cells without stimulation. We performed a double-immunofluorescence staining with anti-TLR9 and ER or endosome markers in GEN2.2 cells or SCARB2 knockdown cells. Confocal microscopy revealed that TLR9 localized in calnexin-positive ER instead of early or late endosomes, prior to stimulation (Fig. 7A). The subcellular distribution of TLR9 was not altered by SCARB2 knockdown in unstimulated cells (data not shown). Then we treated SCARB2 knockdown (sh-1) and control (sh-c) cells with CpG B and intracellularly stained with anti-TLR9 Ab

together with ER or endosome markers. Upon stimulation, TLR9 left ER and moved toward LAMP-1–positive late endosomes (Fig. 7B). The translocation was appreciably detected in 20% of control cells, but much less (5%) was detected in SCARB2 knockdown cells (Fig. 7B, 7C). Therefore, these results show that TLR9 localizes in ER in pDCs and is rapidly recruited to late endosomes upon stimulation in a SCARB2-dependent manner.

## Discussion

In the current study, we have identified an unexpected role of SCARB2 as an important regulator of IFN-I production and a mediator for TLR9 trafficking. The discovery of these functions links together many of the details from previous studies of both SCARB2 and TLR9 trafficking and, importantly, highlights the enormous synergy between vesicle transfer system and antiviral activity in pDCs.

SCARB2 has been very well characterized as a highly glycosylated transmembrane lysosomal resident protein since its discovery in rat liver in 1985 (6). However, early studies have just focused on its subcellular distribution or kinetics, and most of the existing studies remain at biochemistry level or are carried out in cell lines or mouse cells (7–9, 14, 42–44). The nature of how SCARB2 works in human primary cells is largely unknown.

Based on cDNA microarray data, we found that pDCs expressed SCARB2 at the highest level in human peripheral blood compared with other immune cells (Fig. 1A). This result was further confirmed at both RNA and protein level (Fig. 1B, 1C). pDCs are the most potent IFN-producing cells and play a vital role in innate immune responses to viral infections (20, 45). Intracellular TLR7 and TLR9 are selectively expressed in pDCs to recognize viral nucleic acids and rapidly initiate the IFN-I production. IFNs have potent effect on promoting the function of other immune cells, such as NK cells, B cells, T cells, and myeloid DCs during an antiviral immune response. Although innate and adaptive immunity is vital for organisms to resist viral and bacterial infection, it is also important to distinguish self from nonself molecules to avoid autoimmunity. Organisms have evolved a series of precise regulatory mechanisms to prevent TLRs from self-reactivation (46, 47). One of these mechanisms is the subcellular localization and trafficking properties of TLRs. How TLR7 and TLR9 accurately traffic to their destined subcellular compartment and what proteins participate in this process has attracted great interest.

Our results show that SCARB2 mediates TLR9 trafficking from ER to late endosome/lysosome upon CpG B stimulation (Fig. 7B, 7C). Such a finding is supported by the following evidence: First, after synthesized in ER, SCARB2 translocates into late endosome/lysosome and regulates the biogenesis and reorganization of endosomes and lysosomes (7, 9–12, 15). Similarly, TLR9 must traffic into these vesicles to undergo a proteolytic processing and become functional (28, 48). Second, trafficking of SCARB2 and TLR9 between ER and endosome/lysosome is directed by the same adaptor protein AP-3 (27, 42, 49).

Besides AP-3, many other molecules are also involved in the processing and trafficking of TLR9. Heat shock protein gp96 regulates proteolytic processing and conformational stability

of TLR9 and thereby affects its trafficking (50). Biogenesis of lysosome-related organelle complexes BLOC-1, BLOC-2, BLOC-3 (51), and solute carrier protein superfamily member Slc15a4 (52) is also essential for the signaling of TLR9 by interacting with AP-3. Phospholipid scramblase 1 regulates IFN-I responses by directly binding to the leucine-rich repeat domain of TLR9 and directing its trafficking to the endosomal compartment in pDCs (53). All of these proteins, together with SCARB2, may form an intricate and precise system to regulate the function of TLR9. How SCARB2 interacts with those TLR9-involved proteins will be interesting subjects of further studies.

Our results that SCARB2 regulates IFN production in pDCs (Fig. 3D, 3E) would be in keeping with the findings that Carrasco-Marín et al. (14) have demonstrated in SCARB2 knockout mice. In the innate immune response to *Listeria monocytogenes*, SCARB2 was shown to be required for the production of proinflammatory cytokines and chemokines, such as MCP-1, TNF- $\alpha$ , and IL-6, in macrophages. These results together with our findings suggest the important function of SCARB2 in immune system.

However, in response to virus stimulation, SCARB2 knockdown showed no influence on the production of IFN- $\alpha$  or IL-6 (Fig. 4). These results can be explained by the fact that Flu and HSV are recognized by distinct classes of PRRs, not only TLRs, but also some cytosolic sensors. For example, retinoic acid-inducible gene I is crucial for the viral detection and type I IFN production in Flu-infected epithelial cells, conventional DCs, and alveolar macrophages (54). However, in response to HSV infection, DNA-dependent activator of IFN regulatory factor, cyclic guanosine monophosphate-adenosine monophosphate synthase, DDX41, and DNA-dependent protein kinase all can mediate type I IFN induction after sensing viral DNA in the cytosol (55). Therefore, the influence of SCARB2 on type I IFN induction may be compensated by those cytosolic sensor-mediated pathways.

SCARB2 is not the first discovered scavenger receptor that can affect cytokine production and serves as a possible coreceptor for TLRs. Although the role of scavenger receptors in atherogenesis and Alzheimer's disease continues to drive much of the research in this area, their roles in innate immune defense and cytokine responses have received increasing attention.

CD36, another scavenger receptor class B subfamily member, localizes in lipid rafts at the plasma membrane and acts as a coreceptor for TLR2 (56). CD36 serves as a facilitator associating and presenting bacterial lipoteichoic acid as well as diacylated lipo-proteins to TLR2/6 heterodimers in lipid rafts, which triggers the downstream signaling pathway. Subsequently, the whole complex is internalized and targeted to the Golgi apparatus (57). Additionally, Stewart et al. (58) discovered that CD36 also served as a coreceptor for TLR4/6 heterodimers and regulated the expression of proinflammatory cytokines by oxidized low-density lipo-protein and amyloid- $\beta$  peptide stimulations in atherosclerosis and Alzheimer's disease. These results are in agreement with our findings demonstrating that scavenger receptors can play important roles in TLR signaling and immune responses. If SCARB2 and CD36 react with other TLRs just as in the case of CD14, which is a lipid-raft resident protein and works as a coreceptor for a series of TLRs (TLR1/2, TLR2/6, TLR7, and TLR9), will be an interesting subject of further studies (57, 59).

Our findings that SCARB2 knockdown cells responded differently to the two types of CpG-ODNs are surprising. In response to CpG B, IFN-I production was sharply diminished in knockdown cells (Fig. 3D, 3E). In response to CpG A, SCARB2 seemed to be dispensable for IFN production (Fig. 3C). Such a contradiction can be explained by the possibility that CpG A and CpG B have distinct trafficking pathways to activate pDCs and SCARB2 is only involved in the process of CpG B stimulation. This possibility is in agreement with findings from several other studies. CpG A and CpG B have different primary sequence motifs as well as secondary and tertiary structures and behave differently in IFN- $\alpha$  production and pDC maturation according to their subcellular localization. CpG A contains poly-G tails that enable the formation of aggregated multimeric structures. This makes it preferentially retained in early endosomes, correlating with high IFN- $\alpha$  production but inefficient stimulation of costimulatory molecule expression. In contrast, single-stranded CpG B travels quickly into late endosomes (Fig. 6C) and induces strong pDC maturation but weaker IFN- $\alpha$  secretion (30, 31). Others' research and our results clearly demonstrate that SCARB2 localizes in late endosome/lysosome and plays a critical role in endolysosome biogenesis. According to this, we speculate that, when this protein is knockdown, internal environment such as pH or acid proteolytic enzyme function in late endosome/lysosome is damaged, which impairs CpG B downstream signaling. In the case of CpG A, early endosome is not influenced by SCARB2 knockdown; thus, CpG A-induced IFN production is not impaired.

Meanwhile, we generated SCARB2-overexpressed GEN2.2 cells and monitored the IFN- $\alpha$  production in response to both CpG-ODNs. IFN- $\alpha$  production was sharply decreased with SCARB2 overexpression upon CpG A/B stimulation (data not shown), which was in agreement with the findings of other studies demonstrating that overexpression of SCARB2 would cause an enlargement of both early and late endosome and an impairment of endocytic membrane trafficking (12, 15).

Technically, it has been very challenging to directly study the function of SCARB2 in pDCs because of the difficulty in obtaining a large number of pDCs from human tissues or tissue cultures as well as the paucity and vulnerability of primary pDCs. Nevertheless, we once tried to knock down SCARB2 in primary pDCs by transducing shRNA into the cells by electrotransfection or Lipofectamine. Unfortunately, both kinds of operations activated pDCs and caused a significant upregulation of SCARB2 (data not shown). Because there were technical challenges to knock down SCARB2 in primary pDCs, we settled for the pDC cell line GEN2.2 in our research.

A recent report has shown that pDCs suffer massive reductions in patients with GD, which is a rare autosomal recessive disorder having a close relationship with  $\beta$ -GC or SCARB2 deficiency. pDCs from GD patients exhibit a dysfunction in IFN- $\alpha$  production after TLR9 stimulation, resulting in a decreased response to pathogens (60). Previous studies have demonstrated that SCARB2 works as a receptor for  $\beta$ -GC and helps to transport this lysosomal hydrolase from ER to lysosome (16). GD results from the inherited deficiency of  $\beta$ -GC, which cleaves the glycolipid glucocerebroside into glucose and ceramide (61). In recent years, an increasing number of groups report that mutations in SCARB2 can cause progressive myoclonus epilepsies or action myoclonus-renal failure, which has similar phenotypes with GD (62, 63). It is possible that mutations in  $\beta$ -GC or SCARB2 lead to

enzyme dysfunction, and, as a result, glucosylceramide accumulates in lysosome and impairs endocytic system, which further blocks TLR9 trafficking and IFN- $\alpha$  production.

In addition, TLR9 has been reported to be linked to autoimmune diseases such as systemic lupus erythematosus (64). Our finding that SCARB2 is required for TLR9-dependent IFN production toward CpG DNA stimulation offers the possibility that SCARB2 may contribute to DNA-mediated immune response and autoimmune processes. Therefore, it will be important to further dissect the activities of SCARB2 in TLR9-mediated adjuvant effects in anticancer and antiviral therapies.

## Supplementary Material

Refer to Web version on PubMed Central for supplementary material.

## Acknowledgments

This work was supported by Beijing Municipal Science and Technology Commission Grant SCW 2014-09, Chinese Academy of Science Grant KJZD-EW-L10-02, and Ministry of Health Grant 2013ZX10001002 (to L.Z.).

We thank the Center for Biological Imaging, Institute of Biophysics, Chinese Academy of Science, for confocal microscopy work.

## Abbreviations used in this article

<b>AP</b>	adaptor protein complex
<b>CpG-ODN</b>	CpG oligodeoxynucleotide
<b>ER</b>	endoplasmic reticulum
<b><math>\beta</math>-GC</b>	$\beta$ -glucocerebrosidase
<b>GD</b>	Gaucher disease
<b>IRF</b>	IFN regulatory factor
<b>LAMP</b>	lysosome-associated membrane protein
<b>LMP</b>	lysosomal membrane protein
<b>pDC</b>	plasmacytoid dendritic cell
<b>PRR</b>	pattern recognition receptor
<b>SCARB2</b>	scavenger receptor class B, member 2
<b>shRNA</b>	short hairpin RNA
<b>TfR</b>	transferrin receptor

## References

1. Kornfeld S, Mellman I. The biogenesis of lysosomes. *Annu Rev Cell Biol.* 1989; 5:483–525. [PubMed: 2557062]
2. Mellman I. Endocytosis and molecular sorting. *Annu Rev Cell Dev Biol.* 1996; 12:575–625. [PubMed: 8970738]

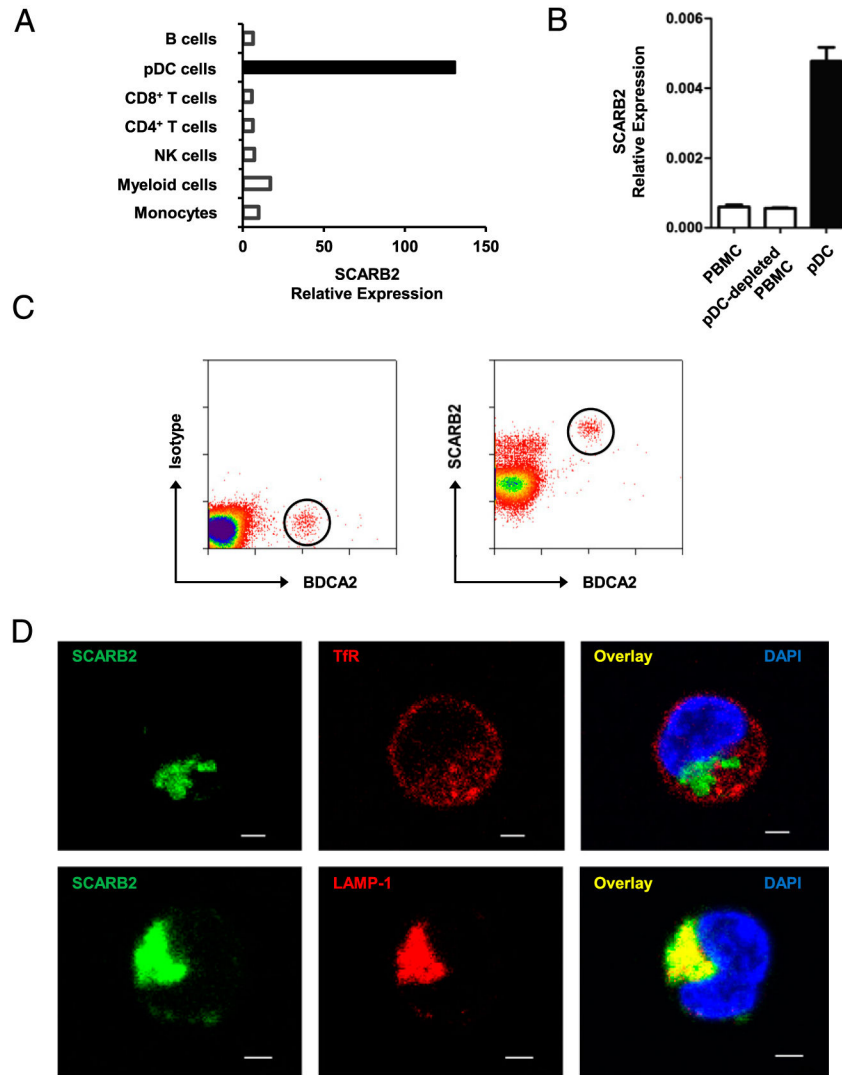
3. de Duve C. Lysosomes revisited. *Eur J Biochem.* 1983; 137:391–397. [PubMed: 6319122]
4. Schröder B, Wrocklage C, Pan C, Jäger R, Kösters B, Schäfer H, Elsässer HP, Mann M, Hasilik A. Integral and associated lysosomal membrane proteins. *Traffic.* 2007; 8:1676–1686. [PubMed: 17897319]
5. Peiser L, Mukhopadhyay S, Gordon S. Scavenger receptors in innate immunity. *Curr Opin Immunol.* 2002; 14:123–128. [PubMed: 11790542]
6. Lewis V, Green SA, Marsh M, Vihko P, Helenius A, Mellman I. Glycoproteins of the lysosomal membrane. *J Cell Biol.* 1985; 100:1839–1847. [PubMed: 3922993]
7. Barriocanal JG, Bonifacino JS, Yuan L, Sandoval IV. Biosynthesis, glycosylation, movement through the Golgi system, and transport to lysosomes by an N-linked carbohydrate-independent mechanism of three lysosomal integral membrane proteins. *J Biol Chem.* 1986; 261:16755–16763. [PubMed: 3782140]
8. Ogata S, Fukuda M. Lysosomal targeting of LIMP II membrane glycoprotein requires a novel Leu-Ile motif at a particular position in its cytoplasmic tail. *J Biol Chem.* 1994; 269:5210–5217. [PubMed: 8106503]
9. Sandoval IV, Arredondo JJ, Alcalde J, Gonzalez Noriega A, Vandekerckhove J, Jimenez MA, Rico M. The residues Leu(Ile) 475-Ile(Leu, Val, Ala)476, contained in the extended carboxyl cytoplasmic tail, are critical for targeting of the resident lysosomal membrane protein LIMP II to lysosomes. *J Biol Chem.* 1994; 269:6622–6631. [PubMed: 7509809]
10. Höning S, Sandoval IV, von Figura K. A di-leucine-based motif in the cytoplasmic tail of LIMP-II and tyrosinase mediates selective binding of AP-3. *EMBO J.* 1998; 17:1304–1314. [PubMed: 9482728]
11. Janvier K, Kato Y, Boehm M, Rose JR, Martina JA, Kim BY, Venkatesan S, Bonifacino JS. Recognition of dileucine-based sorting signals from HIV-1 Nef and LIMP-II by the AP-1 gamma-sigma1 and AP-3 delta-sigma3 hemicomplexes. *J Cell Biol.* 2003; 163:1281–1290. [PubMed: 14691137]
12. Kuronita T, Eskelinen EL, Fujita H, Saftig P, Himeno M, Tanaka Y. A role for the lysosomal membrane protein LGP85 in the biogenesis and maintenance of endosomal and lysosomal morphology. *J Cell Sci.* 2002; 115:4117–4131. [PubMed: 12356916]
13. Yamayoshi S, Yamashita Y, Li J, Hanagata N, Minowa T, Takemura T, Koike S. Scavenger receptor B2 is a cellular receptor for enterovirus 71. *Nat Med.* 2009; 15:798–801. [PubMed: 19543282]
14. Carrasco-Marín E, Fernández-Prieto L, Rodríguez-Del Río E, Madrazo-Toca F, Reinheckel T, Saftig P, Alvarez-Dominguez C. LIMP-2 links late phagosomal trafficking with the onset of the innate immune response to *Listeria monocytogenes*: a role in macrophage activation. *J Biol Chem.* 2011; 286:3332–3341. [PubMed: 21123180]
15. Kuronita T, Hatano T, Furuyama A, Hirota Y, Masuyama N, Saftig P, Himeno M, Fujita H, Tanaka Y. The NH(2)-terminal transmembrane and lumenal domains of LGP85 are needed for the formation of enlarged endosomes/lysosomes. *Traffic.* 2005; 6:895–906. [PubMed: 16138903]
16. Reczek D, Schwake M, Schröder J, Hughes H, Blanz J, Jin X, Brondyk W, Van Patten S, Edmunds T, Saftig P. LIMP-2 is a receptor for lysosomal mannose-6-phosphate-independent targeting of beta-glucoocerebrosidase. *Cell.* 2007; 131:770–783. [PubMed: 18022370]
17. Yamayoshi S, Ohka S, Fujii K, Koike S. Functional comparison of SCARB2 and PSGL1 as receptors for enterovirus 71. *J Virol.* 2013; 87:3335–3347. [PubMed: 23302872]
18. Yamayoshi S, Iizuka S, Yamashita T, Minagawa H, Mizuta K, Okamoto M, Nishimura H, Sanjoh K, Katsushima N, Itagaki T, et al. Human SCARB2-dependent infection by coxsackievirus A7, A14, and A16 and enterovirus 71. *J Virol.* 2012; 86:5686–5696. [PubMed: 22438546]
19. Baranova IN, Vishnyakova TG, Bocharov AV, Leelahavanichkul A, Kurlander R, Chen Z, Souza AC, Yuen PS, Star RA, Csako G, et al. Class B scavenger receptor types I and II and CD36 mediate bacterial recognition and proinflammatory signaling induced by *Escherichia coli*, lipopolysaccharide, and cytosolic chaperonin 60. *J Immunol.* 2012; 188:1371–1380. [PubMed: 22205027]
20. Liu YJ. IPC: professional type 1 interferon-producing cells and plasmacytoid dendritic cell precursors. *Annu Rev Immunol.* 2005; 23:275–306. [PubMed: 15771572]



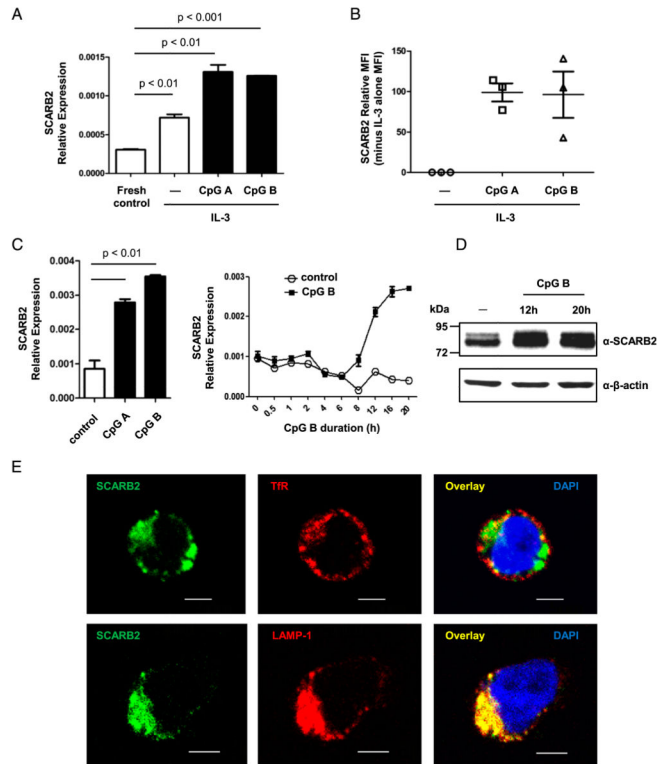
21. Asselin-Paturel C, Trinchieri G. Production of type I interferons: plasmacytoid dendritic cells and beyond. *J Exp Med*. 2005; 202:461–465. [PubMed: 16103406]
22. Barton GM, Kagan JC, Medzhitov R. Intracellular localization of Toll-like receptor 9 prevents recognition of self DNA but facilitates access to viral DNA. *Nat Immunol*. 2006; 7:49–56. [PubMed: 16341217]
23. Fukui R, Saitoh S, Kanno A, Onji M, Shibata T, Ito A, Onji M, Matsumoto M, Akira S, Yoshida N, Miyake K. UNC93B1 restricts systemic lethal inflammation by orchestrating Toll-like receptor 7 and 9 trafficking. *Immunity*. 2011; 35:69–81. [PubMed: 21683627]
24. Kim YM, Brinkmann MM, Paquet ME, Ploegh HL. UNC93B1 delivers nucleotide-sensing Toll-like receptors to endolysosomes. *Nature*. 2008; 452:234–238. [PubMed: 18305481]
25. Fukui R, Saitoh S, Matsumoto F, Kozuka-Hata H, Oyama M, Tabeta K, Beutler B, Miyake K. UNC93B1 biases Toll-like receptor responses to nucleic acid in dendritic cells toward DNA- but against RNA-sensing. *J Exp Med*. 2009; 206:1339–1350. [PubMed: 19451267]
26. Lee BL, Moon JE, Shu JH, Yuan L, Newman ZR, Schekman R, Barton GM. UNC93B1 mediates differential trafficking of endosomal TLRs. *eLife*. 2013; 2:e00291. Available at: <http://elifesciences.org/content/2/e00291>. [PubMed: 23426999]
27. Sasai M, Linehan MM, Iwasaki A. Bifurcation of Toll-like receptor 9 signaling by adaptor protein 3. *Science*. 2010; 329:1530–1534. [PubMed: 20847273]
28. Park B, Brinkmann MM, Spooner E, Lee CC, Kim YM, Ploegh HL. Proteolytic cleavage in an endolysosomal compartment is required for activation of Toll-like receptor 9. *Nat Immunol*. 2008; 9:1407–1414. [PubMed: 18931679]
29. Sepulveda FE, Maschalidi S, Colisson R, Heslop L, Ghirelli C, Sakka E, Lennon-Duménil AM, Amigorena S, Cabanie L, Manoury B. Critical role for asparagine endopeptidase in endocytic Toll-like receptor signaling in dendritic cells. *Immunity*. 2009; 31:737–748. [PubMed: 19879164]
30. Kerkmann M, Rothenfusser S, Hornung V, Towarowski A, Wagner M, Sarris A, Giese T, Endres S, Hartmann G. Activation with CpG-A and CpG-B oligonucleotides reveals two distinct regulatory pathways of type I IFN synthesis in human plasmacytoid dendritic cells. *J Immunol*. 2003; 170:4465–4474. [PubMed: 12707322]
31. Guiducci C, Ott G, Chan JH, Damon E, Calacsan C, Matray T, Lee KD, Coffman RL, Barrat FJ. Properties regulating the nature of the plasmacytoid dendritic cell response to Toll-like receptor 9 activation. *J Exp Med*. 2006; 203:1999–2008. [PubMed: 16864658]
32. Hoshino K, Sugiyama T, Matsumoto M, Tanaka T, Saito M, Hemmi H, Ohara O, Akira S, Kaisho T. IkappaB kinase-alpha is critical for interferon-alpha production induced by Toll-like receptors 7 and 9. *Nature*. 2006; 440:949–953. [PubMed: 16612387]
33. Honda K, Ohba Y, Yanai H, Negishi H, Mizutani T, Takaoka A, Taya C, Taniguchi T. Spatiotemporal regulation of MyD88-IRF-7 signalling for robust type-I interferon induction. *Nature*. 2005; 434:1035–1040. [PubMed: 15815647]
34. Honda K, Yanai H, Negishi H, Asagiri M, Sato M, Mizutani T, Shimada N, Ohba Y, Takaoka A, Yoshida N, Taniguchi T. IRF-7 is the master regulator of type-I interferon-dependent immune responses. *Nature*. 2005; 434:772–777. [PubMed: 15800576]
35. Villadangos JA, Young L. Antigen-presentation properties of plasmacytoid dendritic cells. *Immunity*. 2008; 29:352–361. [PubMed: 18799143]
36. Chaperot L, Perrot I, Jacob MC, Blanchard D, Salaun V, Deneys V, Lebecque S, Brière F, Bensa JC, Plumas J. Leukemic plasmacytoid dendritic cells share phenotypic and functional features with their normal counterparts. *Eur J Immunol*. 2004; 34:418–426. [PubMed: 14768046]
37. Mulcahy JV, Riddell DR, Owen JS. Human scavenger receptor class B type II (SR-BII) and cellular cholesterol efflux. *Biochem J*. 2004; 377:741–747. [PubMed: 14570588]
38. Pauls E, Shpiro N, Peggie M, Young ER, Sorcek RJ, Tan L, Choi HG, Cohen P. Essential role for IKK $\beta$  in production of type I interferons by plasmacytoid dendritic cells. *J Biol Chem*. 2012; 287:19216–19228. [PubMed: 22511786]
39. Di Domizio J, Blum A, Gallagher-Gambarelli M, Molens JP, Chaperot L, Plumas J. TLR7 stimulation in human plasmacytoid dendritic cells leads to the induction of early IFN-inducible genes in the absence of type I IFN. *Blood*. 2009; 114:1794–1802. [PubMed: 19553637]

40. Honda K, Takaoka A, Taniguchi T. Type I interferon [corrected] gene induction by the interferon regulatory factor family of transcription factors. *Immunity*. 2006; 25:349–360. [PubMed: 16979567]
41. Honda K, Taniguchi T. IRFs: master regulators of signalling by Toll-like receptors and cytosolic pattern-recognition receptors. *Nat Rev Immunol*. 2006; 6:644–658. [PubMed: 16932750]
42. Le Borgne R, Alconada A, Bauer U, Hoflack B. The mammalian AP-3 adaptor-like complex mediates the intracellular transport of lysosomal membrane glycoproteins. *J Biol Chem*. 1998; 273:29451–29461. [PubMed: 9792650]
43. Gamp AC, Tanaka Y, Lüllmann-Rauch R, Wittke D, D’Hooge R, De Deyn PP, Moser T, Maier H, Hartmann D, Reiss K, et al. LIMP-2/LGP85 deficiency causes ureteric pelvic junction obstruction, deafness and peripheral neuropathy in mice. *Hum Mol Genet*. 2003; 12:631–646. [PubMed: 12620969]
44. Knipper M, Claussen C, Rüttiger L, Zimmermann U, Lüllmann-Rauch R, Eskelinen EL, Schröder J, Schwake M, Saftig P. Deafness in LIMP2-deficient mice due to early loss of the potassium channel KCNQ1/KCNE1 in marginal cells of the stria vascularis. *J Physiol*. 2006; 576:73–86. [PubMed: 16901941]
45. Colonna M, Trinchieri G, Liu YJ. Plasmacytoid dendritic cells in immunity. *Nat Immunol*. 2004; 5:1219–1226. [PubMed: 15549123]
46. Krutzik SR, Sieling PA, Modlin RL. The role of Toll-like receptors in host defense against microbial infection. *Curr Opin Immunol*. 2001; 13:104–108. [PubMed: 11154925]
47. Marshak-Rothstein A. Toll-like receptors in systemic autoimmune disease. *Nat Rev Immunol*. 2006; 6:823–835. [PubMed: 17063184]
48. Latz E, Schoenemeyer A, Visintin A, Fitzgerald KA, Monks BG, Knetter CF, Lien E, Nilsen NJ, Espevik T, Golenbock DT. TLR9 signals after translocating from the ER to CpG DNA in the lysosome. *Nat Immunol*. 2004; 5:190–198. [PubMed: 14716310]
49. Mantegazza AR, Guttentag SH, El-Benna J, Sasai M, Iwasaki A, Shen H, Laufer TM, Marks MS. Adaptor protein-3 in dendritic cells facilitates phagosomal Toll-like receptor signaling and antigen presentation to CD4(+) T cells. *Immunity*. 2012; 36:782–794. [PubMed: 22560444]
50. Brooks JC, Sun W, Chiosis G, Leifer CA. Heat shock protein gp96 regulates Toll-like receptor 9 proteolytic processing and conformational stability. *Biochem Biophys Res Commun*. 2012; 421:780–784. [PubMed: 22554506]
51. Di Pietro SM, Falcón-Pérez JM, Tenza D, Setty SR, Marks MS, Raposo G, Dell’Angelica EC. BLOC-1 interacts with BLOC-2 and the AP-3 complex to facilitate protein trafficking on endosomes. *Mol Biol Cell*. 2006; 17:4027–4038. [PubMed: 16837549]
52. Blasius AL, Arnold CN, Georgel P, Rutschmann S, Xia Y, Lin P, Ross C, Li X, Smart NG, Beutler B. Slc15a4, AP-3, and Hermansky-Pudlak syndrome proteins are required for Toll-like receptor signaling in plasmacytoid dendritic cells. *Proc Natl Acad Sci USA*. 2010; 107:19973–19978. [PubMed: 21045126]
53. Talukder AH, Bao M, Kim TW, Facchinetti V, Hanabuchi S, Bover L, Zal T, Liu YJ. Phospholipid scramblase 1 regulates Toll-like receptor 9-mediated type I interferon production in plasmacytoid dendritic cells. *Cell Res*. 2012; 22:1129–1139. [PubMed: 22453241]
54. Kato H, Sato S, Yoneyama M, Yamamoto M, Uematsu S, Matsui K, Tsujimura T, Takeda K, Fujita T, Takeuchi O, Akira S. Cell type-specific involvement of RIG-I in antiviral response. *Immunity*. 2005; 23:19–28. [PubMed: 16039576]
55. Ma Y, He B. Recognition of herpes simplex viruses: Toll-like receptors and beyond. *J Mol Biol*. 2014; 426:1133–1147. [PubMed: 24262390]
56. Hoebe K, Georgel P, Rutschmann S, Du X, Mudd S, Crozat K, Sovath S, Shamel L, Hartung T, Zähringer U, Beutler B. CD36 is a sensor of diacylglycerides. *Nature*. 2005; 433:523–527. [PubMed: 15690042]
57. Triantafilou M, Gamper FG, Haston RM, Mouratis MA, Morath S, Hartung T, Triantafilou K. Membrane sorting of Toll-like receptor (TLR)-2/6 and TLR2/1 heterodimers at the cell surface determines heterotypic associations with CD36 and intracellular targeting. *J Biol Chem*. 2006; 281:31002–31011. [PubMed: 16880211]

58. Stewart CR, Stuart LM, Wilkinson K, van Gils JM, Deng J, Halle A, Rayner KJ, Boyer L, Zhong R, Frazier WA, et al. CD36 ligands promote sterile inflammation through assembly of a Toll-like receptor 4 and 6 heterodimer. *Nat Immunol.* 2010; 11:155–161. [PubMed: 20037584]
59. Baumann CL, Aspalter IM, Sharif O, Pichlmair A, Blüml S, Grebien F, Bruckner M, Pasierbek P, Aumayr K, Planyavsky M, et al. CD14 is a coreceptor of Toll-like receptors 7 and 9. *J Exp Med.* 2010; 207:2689–2701. [PubMed: 21078886]
60. Braudeau C, Graveleau J, Rimbart M, Néel A, Hamidou M, Grosbois B, Besançon A, Giraudet S, Terrien C, Josien R, Masseau A. Altered innate function of plasmacytoid dendritic cells restored by enzyme replacement therapy in Gaucher disease. *Blood Cells Mol Dis.* 2013; 50:281–288. [PubMed: 23357793]
61. Beutler E. Gaucher disease: multiple lessons from a single gene disorder. *Acta Paediatr Suppl.* 2006; 95:103–109. [PubMed: 16720474]
62. Dibbens LM, Karakis I, Bayly MA, Costello DJ, Cole AJ, Berkovic SF. Mutation of SCARB2 in a patient with progressive myoclonus epilepsy and demyelinating peripheral neuropathy. *Arch Neurol.* 2011; 68:812–813. [PubMed: 21670406]
63. Velayati A, DePaolo J, Gupta N, Choi JH, Moaven N, Westbroek W, Goker-Alpan O, Goldin E, Stubblefield BK, Kolodny E, et al. A mutation in SCARB2 is a modifier in Gaucher disease. *Hum Mutat.* 2011; 32:1232–1238. [PubMed: 21796727]
64. Krieg AM, Vollmer J. Toll-like receptors 7, 8, and 9: linking innate immunity to autoimmunity. *Immunol Rev.* 2007; 220:251–269. [PubMed: 17979852]

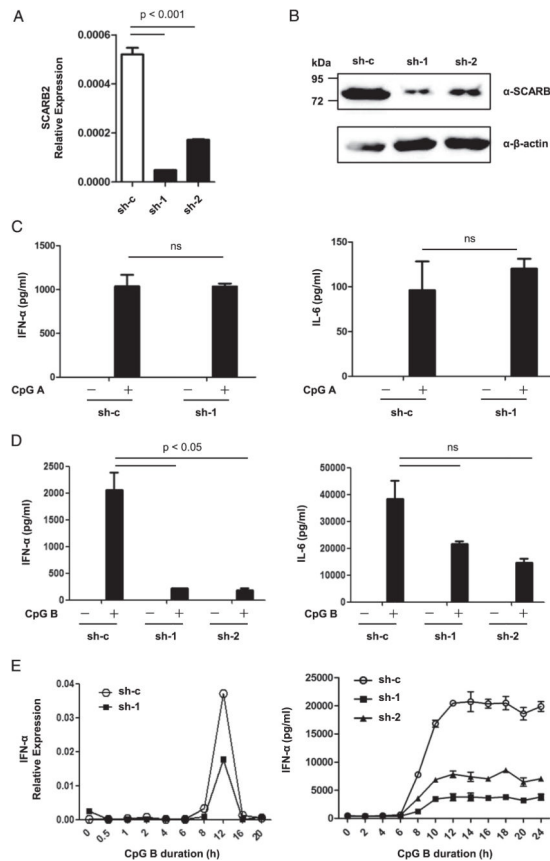
**FIGURE 1.**

SCARB2 is preferentially expressed in pDCs and localizes in late endosome/lysosome. **(A)** The expression profile of SCARB2 in human leukocytes based on cDNA data. **(B)** Human PBMCs, pDC-depleted PBMCs, and pDCs were isolated from healthy volunteers. The level of SCARB2 transcript was quantified by real-time PCR and normalized with GAPDH. **(C)** Intracellular FACS staining of SCARB2 was carried out in human PBMCs. pDCs are identified by their BDCA2 expression (circled). Matched isotype IgG was used as a control (*left panel*). **(D)** Purified pDCs were stained intracellularly with anti-SCARB2 and early (*upper panel*) or late (*lower panel*) endosome markers. The subcellular distribution of SCARB2 was shown by confocal microscopy. Nucleus was stained by DAPI (blue). Results are representative of at least three independent experiments. Scale bars, 5  $\mu$ m.

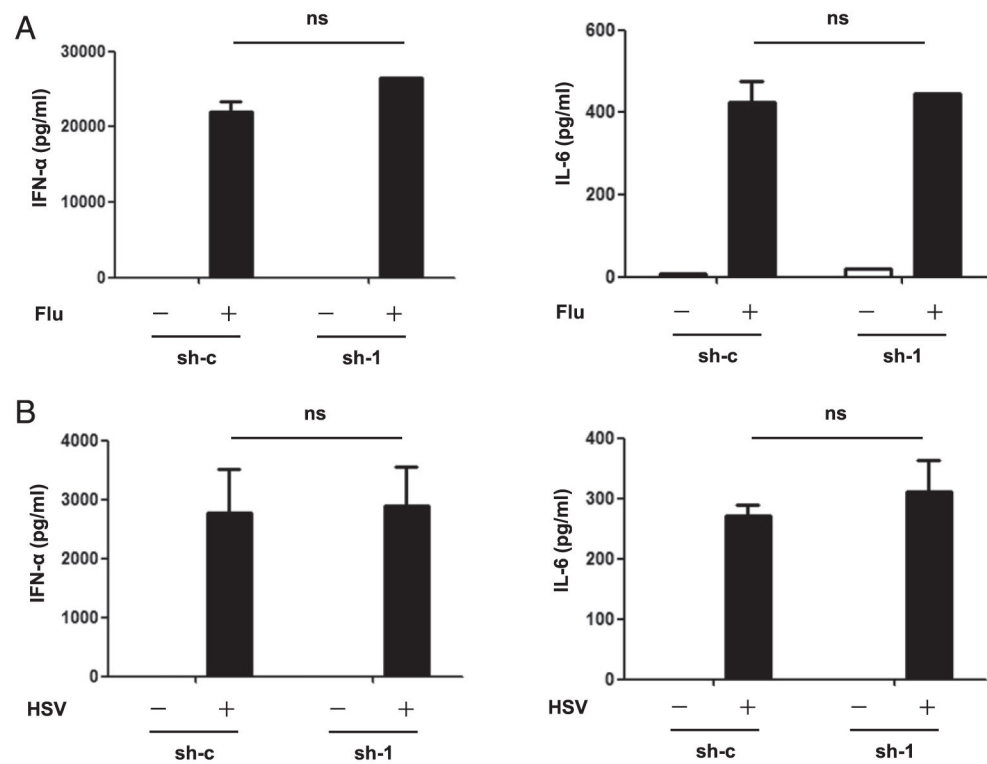


**FIGURE 2.**

CpG induces upregulation of SCARB2 expression in pDCs. (A and B) Purified pDCs were stimulated with CpG A/B in presence of IL-3 for 20 h. (A) The level of SCARB2 transcript was determined using real-time PCR and normalized with EF1- $\alpha$  as a housekeeping control. (B) pDCs were intracellularly stained with anti-SCARB2, and the mean fluorescence intensity (MFI) of stimulated samples was normalized relative to the none-CpG control cells (SCARB2 relative MFI = sample MFI minus none-CpG control MFI). Each symbol represents one independent experiment. (C–E) GEN2.2 cells were activated by CpG A/B for the indicated durations. (C) The level of SCARB2 transcript was determined using real-time PCR and normalized with GAPDH as a housekeeping control. (D) After 12- and 20-h stimulation, cells were lysed and analyzed by Western blotting with anti-SCARB2.  $\beta$ -actin levels are shown as loading controls. (E) After 20-h stimulation, cells were stained intracellularly with anti-SCARB2 and early (*upper panel*) or late (*lower panel*) endosome markers. The subcellular distribution of SCARB2 was shown by confocal microscopy. Nucleus was stained by DAPI (blue). Results are representative of at least three independent experiments. The data are presented as the mean  $\pm$  SEM of duplicates. Scale bars, 5  $\mu$ m.

**FIGURE 3.**

SCARB2 regulates TLR9-dependent IFN-I production. (A and B) GEN2.2 cells were transduced with lentivirus carrying either scrambled shRNA (sh-c) or shRNA targeting SCARB2 (sh-1/2), and stable cell lines were generated. The knockdown efficiency was confirmed by real-time PCR (A) and Western blotting (B). GAPDH or  $\beta$ -actin was used as a housekeeping control, respectively. SCARB2 knockdown (sh-1/2) and control cells (sh-c) were stimulated with CpG A (C) or CpG B (D) for 20 h. Levels of IFN- $\alpha$  (left panel) and IL-6 (right panel) in the culture supernatants were measured by ELISA. (E) SCARB2 knockdown (sh-1/2) and control cells (sh-c) were stimulated with CpG B for the indicated durations. Cells were collected, and the levels of IFN- $\alpha$  transcript were detected by real-time PCR normalized with GAPDH as a housekeeping control (left panel). Levels of IFN- $\alpha$  in the culture supernatants were measured by ELISA (right panel). Results are representative of at least three independent experiments. The data are presented as the mean  $\pm$  SEM of duplicates (ns indicates not significant).

**FIGURE 4.**

SCARB2 is not required for virus-induced IFN-I production. SCARB2 knockdown (sh-1) and control cells (sh-c) were stimulated with Flu (A) and HSV (B) for 22 h. Levels of IFN- $\alpha$  (left panel) and IL-6 (right panel) in the culture supernatants were measured by ELISA. Results are representative of at least three independent experiments. The data are presented as the mean  $\pm$  SEM of duplicates. ns, Not significant.

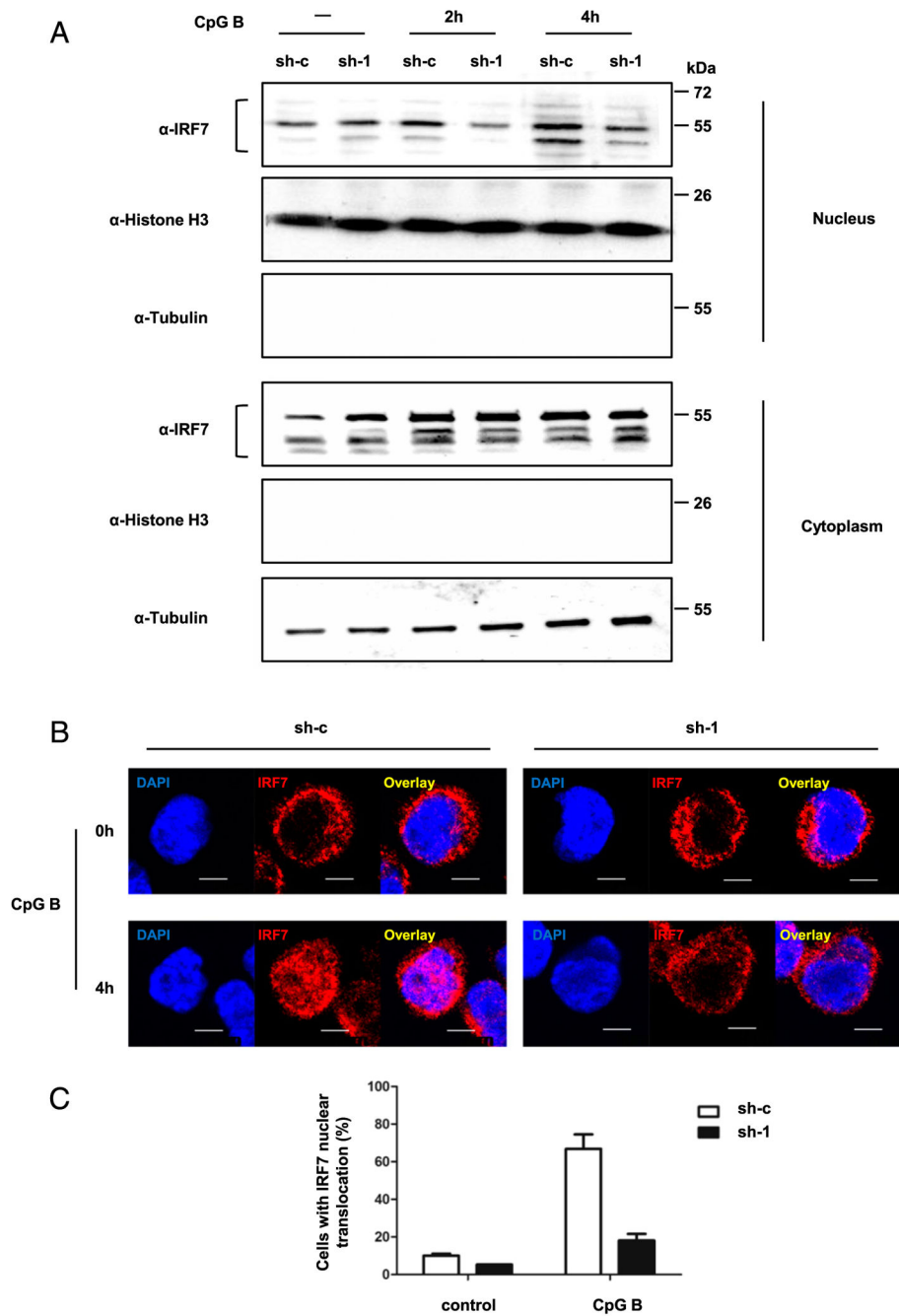


**FIGURE 5.** SCARB2 is essential for TLR9-mediated activation of IRF7. SCARB2 knockdown (sh-1) and control cells (sh-c) were stimulated with CpG B for 2 and 4 h. (A) Nuclear and cytosolic fractions were isolated and immunoblotted with anti-IRF7 Ab. Histone H3 and tubulin were used as nuclear and cytosolic markers, respectively. (B) Cells were stained intracellularly with anti-IRF7. Nucleus was stained by DAPI (blue). The colocalization of IRF7 with nucleus was shown by confocal microscopy. Scale bars, 5  $\mu$ m. (C) The percentage of cells with significant IRF7 nuclear translocation was summarized from random fields of view



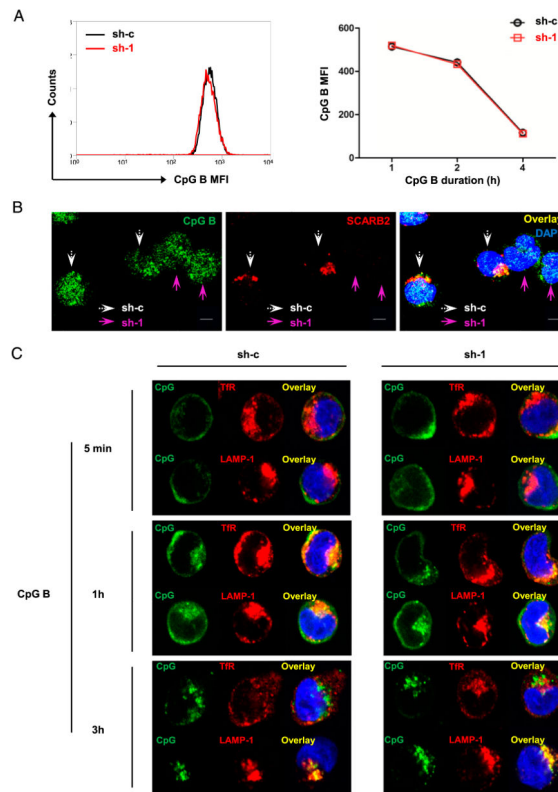
(control samples: 2 views with at least 50 cells; CpG B-stimulated samples: 3 views with at least 200 cells). Results are representative of at least three independent experiments.

Author Manuscript

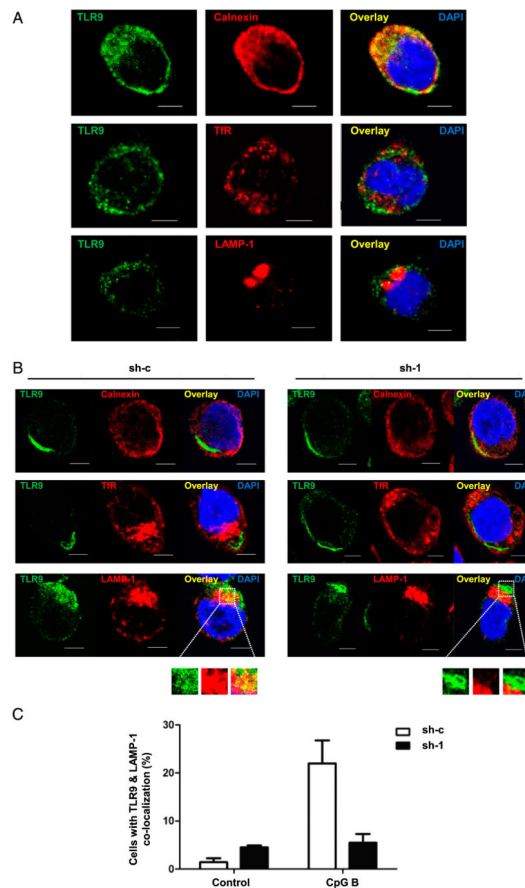
Author Manuscript

Author Manuscript

Author Manuscript

**FIGURE 6.**

SCARB2 is not required for CpG B endocytosis and trafficking. (A) SCARB2 knockdown (sh-1) and control cells (sh-c) were stimulated with biotin-conjugated CpG B. Endocytosis of CpG B was detected by intracellular FACS staining. *Left panel* was a representative histogram of CpG B internalization in control (sh-c, black line) and SCARB2 knockdown cells (sh-1, red line) at 1 h after stimulation. *Right panel* was the summary data of 1, 2, and 4 h post-CpG B stimulation. (B) SCARB2 knockdown (sh-1) and control cells (sh-c) were mixed together with equal amounts and stimulated with biotin-conjugated CpG B for 1 h. Intracellular SCARB2 and CpG B were stained with anti-SCARB2 and Cy5 streptavidin, respectively. White arrows indicate to sh-c control cells, whereas purple arrows indicate to sh-1 SCARB2 knockdown cells. (C) SCARB2 knockdown (sh-1) and control cells (sh-c) were stimulated with biotin-conjugated CpG B for 5 min, 1 h, and 3 h. CpG B trafficking was confirmed by intracellular staining together with early or late endosome marker. Nucleus was stained by DAPI (blue). Results are representative of at least three independent experiments. Scale bars, 5  $\mu$ m.

**FIGURE 7.**

SCARB2 is required for the translocation of TLR9 from ER to late endosomes. **(A)** GEN2.2 cells were stained intracellularly with anti-TLR9 and anti-calnexin (ER, *upper panel*) or anti-Tfr (early endosomes, *middle panel*) or anti-LAMP-1 (late endosomes, *lower panel*). The subcellular distribution of TLR9 was shown by confocal microscopy. Nucleus was stained by DAPI (blue). **(B)** SCARB2 knockdown (sh-1) and control cells (sh-c) were stimulated with CpG B for 4 h. Intracellular TLR9 was stained together with anti-calnexin (*upper panel*) or anti-Tfr (*middle panel*) or anti-LAMP-1 (*lower panel*). The subcellular distribution was shown by confocal microscopy. Nucleus was stained by DAPI (blue). Scale bars, 5 μm. **(C)** The percentage of cells in which TLR9 translocated into late endosomes was summarized from at least five random fields of view with at least 200 cells per sample. Results are representative of at least three independent experiments.